Simulation of Austenite Grain Growth in Continuous Casting

Christian Bernhard, Jürgen Reiter
Christian Doppler Laboratory of Metallurgical Fundamentals of Continuous Casting Processes; University of Leoben; Franz-Josef-Straße 18; 8700 Leoben; Austria, phone: ++43(0)3842/42189-21, fax: ++43(0)3842/402-2202

Hubert Presslinger
voestalpine Stahl GmbH, VOEST-ALPINE-Straße3, 4031 Linz, Austria, phone: ++43-70-6585-5849, fax: ++43-70-6980-2911

Key Words: continuous casting, prior austenite grain size, prediction model, precipitates

ABSTRACT

The formation of cracks on the surface of continuously cast semis is basically attributed to the formation of precipitates, phases or segregates during cooling, particularly detrimental along austenite grain boundaries. Coarse columnar austenite grains are known to increase the severity of crack formation [1]. Surface and subsurface cracks are therefore often located below deep oscillation marks (OM) or surface depressions.
Austenite grain growth is mainly influenced by the thermal history, the steel composition and the precipitation of nitrides and carbo-nitrides. The objective of the present work was the development of an austenite grain size prediction model for the slab casting of carbon steels and the implementation in a quality assurance system. In a first step, slabs of different steel grades were investigated to determine the prior austenite grain size. Subsequently, a laboratory experiment was developed to simulate grain growth under conditions close to the continuous casting process. Following extensive experimental and metallographic work, the results served for the validation of a coupled austenite grain growth - precipitation model. The current work focuses on the experimental and numerical simulation of austenite grain growth and presents results for C-Mn-(Al-Nb)-steels.

INTRODUCTION

The present paper addresses the development and validation of a physical and numerical model for predicting the austenite grain size in the continuous casting process. As a benchmark, the prior austenite grain size on the surface of slabs was determined by metallographic examinations for several slabs with varying carbon contents. Additionally, an experiment with columnar solidification was adjusted in order to simulate the cooling conditions in the mold of a slab caster, but also to suppress the precipitation of nitrides and carbonitrides by subsequent accelerated cooling. Thus, it was possible to study the influence of steel composition on the growth of columnar austenite grains.
Finally, the parameters of a grain size prediction model were fitted to the results of the experiment. The resulting model was coupled with a precipitation model and then applied to the slab casting process. The measured and calculated grain size values at the surface and immediately below the surface of the slabs agree very closely.

DETERMINATION OF THE PRIOR AUSTENITE GRAIN SIZE AT THE SURFACE OF SLABS

The determination of the prior austenite grain size at the surface of slabs is time consuming and additionally inaccurate. The local heat transfer at the surface – a dominating parameter for the austenite grain growth – changes continuously within certain limits and varies over the circumference of the slab (e.g. corner, broad face, narrow face). Surface depressions, oscillation marks and local irregularities, such as blown grains [2], might also influence the measured results dramatically. Thus, a statistically sound determination of the prior austenite grain size would demand extensive measurements. The meaningfulness of the results for the validation of a grain growth model would nevertheless be limited as the local cooling conditions are only roughly known.

Within the scope of this work, the efforts on the measurement of austenite grain size at the surface of slabs were therefore limited to answering the following questions:

- Does a significant influence of the steel composition, in particular of carbon, on the prior austenite grain size at the slab surface as indicated by the results of different authors [e.g. 3-7] exist?
- Is the measured grain size in the order of magnitude of published values [8,9]?
- Does the grain size fit with an extrema-distribution [10]?

For the grain size detection, a set of 4 slabs was selected, the composition and main casting parameters are shown in Table I [11]. On every slab, an 18 by 70 mm² area, parallel to the surface and 400 mm off the corner was ground, polished and etched. On every micrograph, a number of at least 200 prior austenite grains was marked by hand and the area of every grain measured by means of a digital image analysis system. This procedure is time consuming but allows both the determination of the grain size distribution and the mean grain size. The details of the metallographic work will be reported elsewhere [12].

Assuming round grains, the diameter of the grain is calculated from the mean grain area, A, with $D = 2 \cdot \sqrt{A/\pi}$ [10]. Table I gives the mean grain diameter at the surface $\overline{D}_0$ and in a distance of 10 mm below the surface, $\overline{D}_{10}$.

Table I: Composition of investigated slabs, main casting parameters and mean measured grain size at the surface and in a distance of 10 mm from the surface [11]

Slab	C, wt.-%	Si, wt.-%	Mn, wt.-%	casting speed, m/min	slab thicknes, mm	slab width, mm	$\overline{D}_0$, mm	$\overline{D}_{10}$, mm
A	0.168	0.21	1.50	1.2	215	1294	0.98	1.78
B	0.185	0.22	0.69	1.2	215	1300	0.71	1.65
C	0.530	0.24	0.86	1.2	215	1171	0.58	0.66
D	0.210	0.22	1.45	1.2	215	1406	0.84	1.52

Figure 1 shows two micrographs of slab A (0.168 wt.-% C, etchant ammonium persulfate) with traced prior austenite grain boundaries at different distances from the surface. The coarsening of the grains with increasing distance from the surface is clearly visible, the average grain diameter amounts to 1.78 (10 mm distance from surface) and 3.24 mm (90 mm distance from surface), respectively.

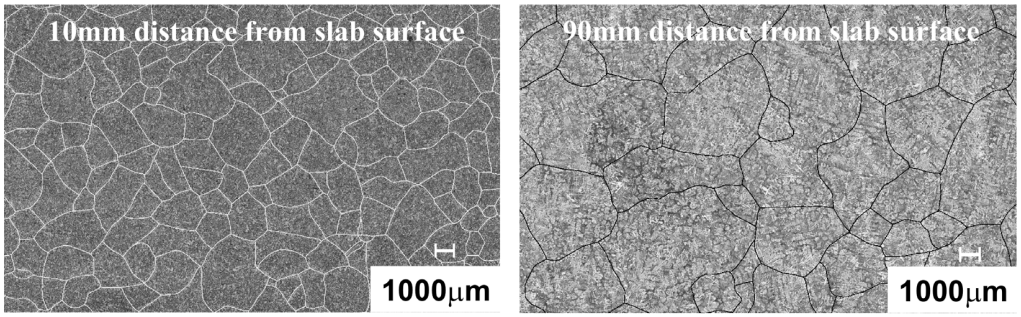

Figure 1: Austenite grain size at two different distances from the slab surface for slab A with 0.168 wt.-% C (etchant: ammonium persulfate) with traced grains [11]

Figure 2 gives an example of the grain size distribution near the surface for slab A and slab C. The measured grain size distribution fits with an extrema distribution. The average grain size amounts to 0.76 mm² for steel A and 0.32 mm² for steel C. Assuming a round grain, the corresponding diameter would be 0.98 and 0.58 mm respectively. The 0.98 mm for steel A and the measured value of 0.71 mm for steel B with a similar composition match well with the published data by Weisgerber et al. [8].

The metallographic examinations of slabs were thus able to answer the questions asked at the beginning. The next step in this work was the development of an experiment in order to simulate austenite grain growth under controlled conditions in the laboratory scale.

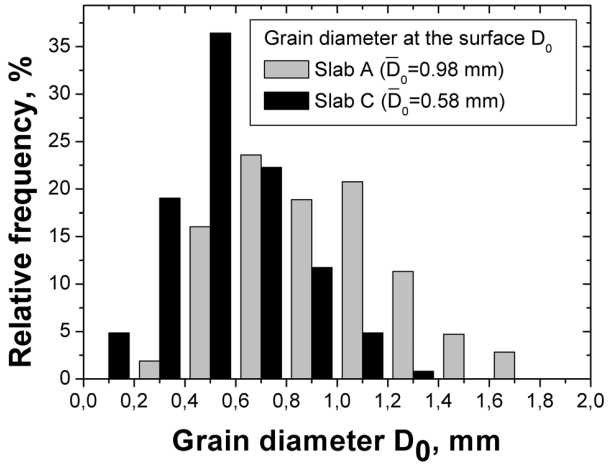

Figure 2: Grain size distribution at the surface for slabs A and C [11]

EXPERIMENTAL WORK

The simulation of austenite grain growth on the surface of the slab necessitates particularly the simulation of the cooling conditions in the mold. The high initial cooling rates result in an early transition from equiaxed to columnar dendritic growth. Only a few millimeters below the surface of the strand, the austenite grains already show a columnar form, oriented towards the center of the slab. The important influence of the solidification structure on the form and size of the austenite grains was already outlined by other authors [e.g. 12] who found an approximate ratio of 5 between the grain diameter and the primary dendrite spacing in distances within 10-80 mm from the surface.

A further reason for the importance of the initial cooling conditions is that the driving force for grain growth follows an Arrhenius term, thus resulting in a clearly higher grain growth rate at higher temperatures. As will be seen from the calculation results later on, the austenite grains attain up to 2/3 of their final grain diameter already at the end of the mold.

A suitable laboratory simulation technique is based on the SSCT-test method [14-16], where a coated substrate is submerged into the liquid melt in an induction furnace, Figure 3. The thickness of the coating controls the intensity of heat extraction from the surface of the solidifying steel shell. This results in a similar characteristic of solidification compared to solidification in a mold.

After a dwell time of 30s, shell and substrate emerge from the melt. The different cooling strategies employed are either quenching in water, accelerated cooling under inert gas atmosphere or cooling in air. After cooling to room temperature, the solidified shell is cut into 16 pieces. Each of these pieces is prepared for metallographic examination and the austenite grain size is determined with the method described above.

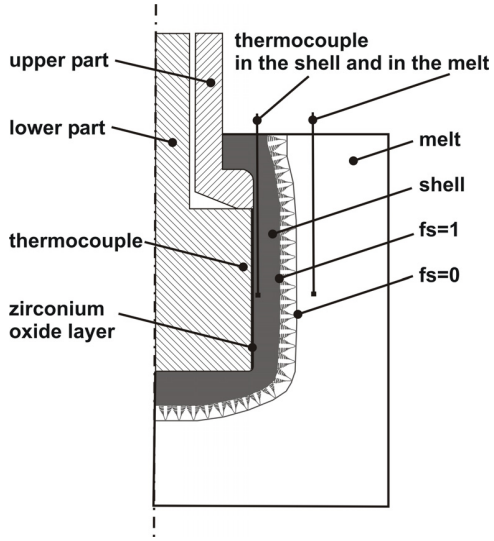

Figure 3: Test body with thermocouples and solidifying shell [10]

The exact control of the thermal conditions during the test is a prerequisite for the analysis of the results. For this purpose, two thermocouples are installed inside the substrate in order to measure the temperature increase. Another thermocouple is positioned inside the solidifying shell. The measured temperatures serve as input data for a thermal model. A typical calculated cooling curve for cooling in air is shown in Figure 4 together with AlN-TTP-characteristics of a steel with 0.059 wt.-% Al and 0.006 wt.-% N. The precipitation of nitrides during the solidification and subsequent cooling is evidently unlikely.

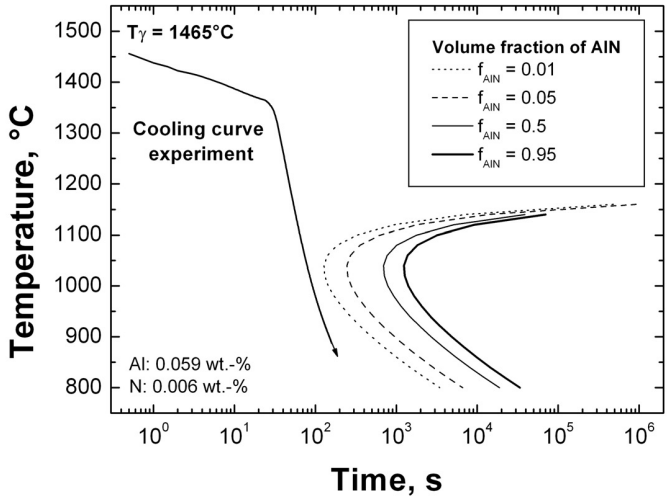

Figure 4: Temperature at the interface between substrate and shell as a function of time for the experiment with subsequent cooling in air and time-temperature-precipitation diagram for steel with 0.059 wt.-% Al and 0.006 wt.-% N [17].

Table II: Chemical composition, measured grain diameter in 1 mm distance from surface $\overline{D}_1$ and T^{γ} for the experiments [11].

Test	C, wt.-%	Si, wt.-%	Mn, wt.-%	cp, wt.-%	$\overline{D}_1$, mm	T^{γ}, °C
A1	0.15	0.21	0.31	0.13	1.29	1470
A2	0.15	0.21	0.30	0.13	1.31	1460
A3	0.45	0.18	0.30	0.44	0.54	1416
A4	0.37	0.19	0.38	0.36	0.55	1433
A5	0.40	0.19	0.32	0.39	0.64	1428
B1	0.05	0.25	1.44	0.07	0.68	1432
B2	0.10	0.26	1.46	0.12	0.99	1453
B3	0.20	0.26	1.45	0.22	0.80	1452
B4	0.51	0.27	1.45	0.53	0.44	1391
B5	0.15	0.21	1.04	0.16	1.29	1468
B6	0.16	0.22	1.88	0.20	0.99	1434
B7	0.08	0.30	1.36	0.09	1.03	1474
B8	0.12	0.28	1.34	0.13	1.11	1460
B9	0.51	0.29	1.28	0.52	0.40	1391
B10	0.70	0.25	1.34	0.72	0.38	1358

The present work illustrates the results of two tests series: The first one with a carbon content between 0.15 and 0.4 wt.-% C, and a Mn-content between 0.30 and 0.38 wt.- %, the second one between 0.05 and 0.70 wt.-% C and between 1.04 and 1.88 wt.-% Mn. The composition of these steels, combined with the calculated equivalent carbon content c_p and the measured mean grain diameter in one millimeter distance from the surface, $\overline{D}_1$ in mm, are given in Table II. The target Al-content was 0.03 wt.-% for all experiments, the highest Al-content is 0.059 wt.-%. The N-content is typically 0.006 wt.-%. T^{γ} denotes the highest temperature of a totally austenitic structure in °C, calculated using the software package IDS.

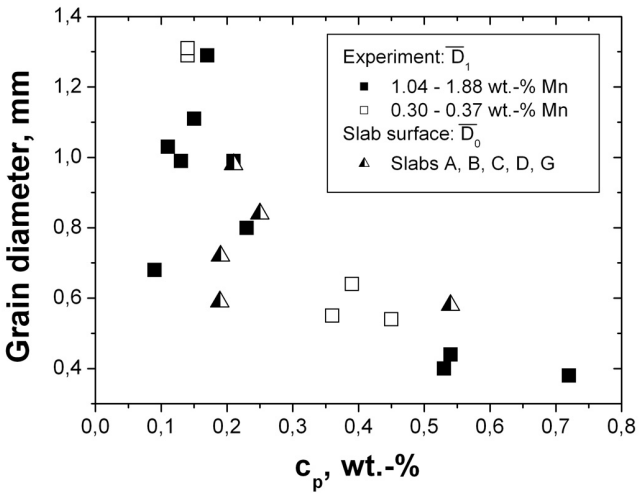

Figure 5: Average grain size $\overline{D}_0$ for all slabs and $\overline{D}_1$ for all laboratory tests vs. equivalent carbon content [11].

Figure 5 illustrates the influence of the equivalent carbon content on $\overline{D}_1$ for all tests. The results show the expected maximum between a c_p of 0.15 and 0.17 wt.-%. The influence of the steel composition is remarkable: Under identical cooling conditions, the final average austenite grain diameter varies by a factor of more than 3. The influence of Mn on the grain size seems to be well explained by its consideration in the calculation of the equivalent carbon content. The measured values are in a similar range as the measured grain size on the slab surface.

AUSTENITE GRAIN SIZE PREDICTION MODEL

According to a model proposed by Andersen and Grong [18], grain growth can be described by the simple differential equation (1) in the presence of pinning particles, where $\overline{D}$ denotes the average grain size and T the temperature in K:

$$\frac{d\overline{D}}{dt} = M_0^{*} \cdot e^{-\frac{Qapp}{R \cdot T}} \cdot \left(\frac{1}{\overline{D}} - \frac{1}{k} \cdot q_p \right)^{\left(\frac{1}{n}-1\right)} \qquad (1)$$

M_0^{*} denotes a kinetic constant that describes the grain boundary mobility in m^2s^{-1}. Q_{app} is the apparent activation energy for grain growth in J/mol and R is the gas constant (8.3145 J/molK). The driving force for grain growth is reciprocal to the actual grain diameter, $\overline{D}$. This driving force is counteracted by a pinning force, exerted by precipitations on the boundary. The term $\frac{k}{q_p}$ represents the maximum grain diameter under normal grain growth conditions, the so-called Zener limit. The time exponent n is a measure of the resistance to grain boundary motion in the presence of impurities and alloying elements in solution [18].
For the analysis of the experimental results, M_0^{*} was assumed with $4 \cdot 10^{-3}$ m^2s^{-1} [7], n with 0.5, the influence of pinning particles was neglected and Q_{app} was used as fitting parameter. The procedure itself is described in detail elsewhere [11, 17], the following dependence between the activation energy and the equivalent carbon content could be found:

$$Q_{app} = 167{,}686 + 40{,}562 \cdot (wt.-\%\ c_p) \qquad (2)$$

The determined correlation results in an excellent correspondence between calculated and measured mean final austenite grain size as shown in Figure 6.

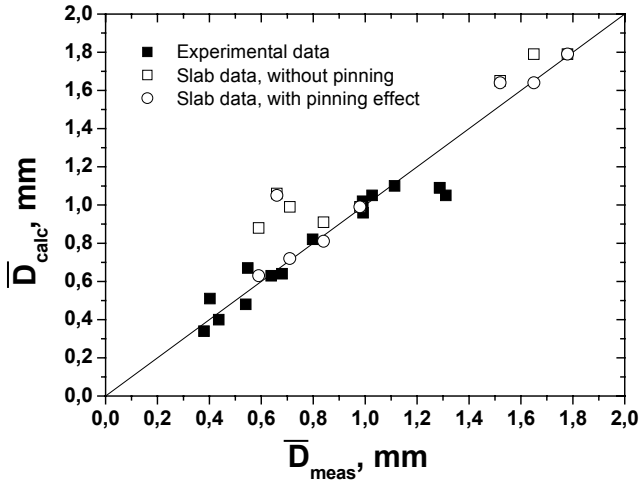

Figure 6: Austenite grain size from the prediction model vs. measured grain size, values from experiment (1 mm below the surface) and slabs (1 and 10 mm below surface).

PREDICTION OF AUSTENITE GRAIN SIZE UNDER CONTINUOUS CASTING CONDITIONS

In contrast with the above described laboratory experiment, precipitations are presumed to play an important role for the austenite grain growth in the cc process. In order to quantify the influence of AlN and Nb(C,N) precipitations on austenite grain growth, the prediction model was coupled with a precipitation model. The background of the model and the thermodynamic and kinetic constants can be taken from [17]. Figure 6 includes the comparison of predicted and measured grain diameter calculated with and without consideration of precipitations. Owing to the pinning effect, the grain diameter decreases up to a maximum of 30% only. For certain combinations of casting speed, secondary cooling conditions and nitride forming element content, precipitations play only a minor role (decrease by 10% or less). The predicted and measured grain diameter (Figure 6) again correspond very well.

The prediction model was finally applied to the question, how far the formation of oscillation marks (OM) at the surface would result in a local increase of the final austenite grain size at the surface of a continuously cast slab? The thermal boundary conditions for the caster were taken from the simulation of a virtual continuous casting machine [19]. The main casting parameters are shown in Table III.

Table III: Data of a virtual caster and main casting parameters [19]

Slab caster	1200 x 250 mm
Casting speed	1.2 and 2.0 m/min
Mold length	800 mm
Overall secondary cooling intensity	0.4 and 0.6 l/kg of steel
8 Cooling zones, % of cooling water	14/36/20/13/8/5/3/1
Roll spacing	Zone I: 202 mm, 25 rolls Zone II, 283 mm, 35 rolls

The geometry of the OM in the simulation was taken from a publication on a comprehensive measurement of the austenite grain size at the surface of slabs [8,9]. Figure 7 shows the “depression type” oscillation mark at the surface with a width of 7 mm and a depth of 0.4 mm. Two different scenarios were assumed for the simulation:

- the gap between OM and mold is either filled with gas, which results in a lower local heat transfer in the mold (gas gap), but a uniform heat transfer along the surface in the secondary cooling zone;
- or the OM is filled with mold powder slag, resulting in a comparably higher heat transfer as long as the slag is liquid, but a higher heat transfer resistance in the secondary cooling zone.

In reality, the oscillation mark will only be partly filled with slag in the mold and only a part of the slag will stick inside the oscillation mark in the secondary cooling zone. The simulation will thus determine the upper and lower limit for the increase of the final austenite grain size. Figure 7 shows the temperature distribution around the oscillation mark at the end of the mold, assuming a casting speed of 1.2 m/min together with the gap between OM and mold being filled with gas. The minimum surface temperature (Position D) amounts to 1065 °C, whereas the temperature in the middle of the OM (Position A) remains at 1140 °C. The thermal history of these points results in an austenite grain size of 510 µm and 670 µm. The increase of the grain diameter at the bottom of the OM amounts to more than 30% at that time.

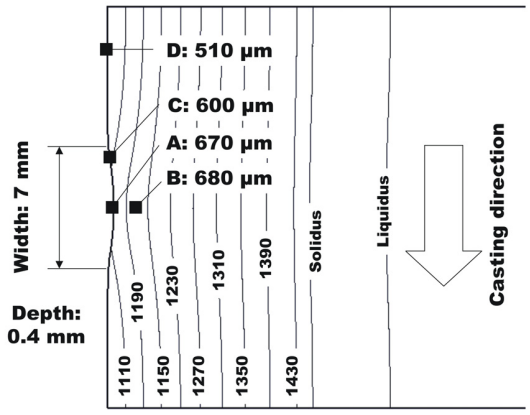

Figure 7: Temperature distribution around an oscillation mark with austenite grain size at the end of the mold

In the simulation the depth of the oscillation mark was varied between 0, 0.05, 0.1, 0.2, 0.4 and 0.6 mm. Figure 8 shows examples for calculated cooling curves at the surface. The lower heat transfer at the bottom of the OM (position A) compared to position D results in a significantly higher surface temperature at the end of the mold. The thermal redistribution below the mold already takes place in the first cooling zones to a large degree. The higher secondary cooling intensity (CW=0.6 l/kg) results in a further decrease of the surface temperature below the mold. Nevertheless, the surface temperature is almost the same at the end of the strand guiding zone for the different cooling intensities and positions at the strand surface.

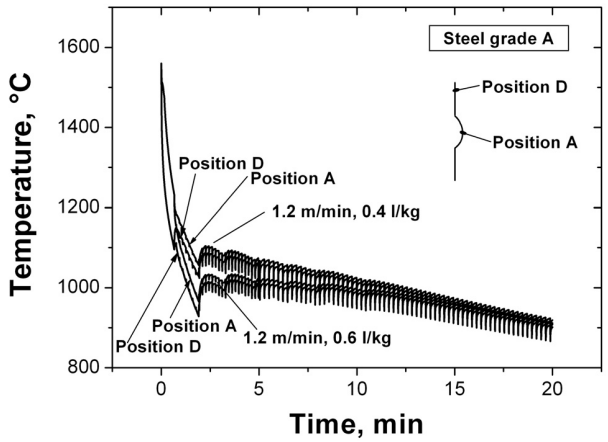

Figure 8: Thermal history on different positions at the surface of a slab

Figure 9 shows the calculated final austenite grain size at the bottom of the oscillation marks vs. depth of the oscillation mark for a steel grade with 0.168 wt.-% C, 0.21 wt.-% Si, 1.5 wt.-% Mn, 0.032 wt.-% Al and 0.004 wt.-% N (steel grade A in Table I).
For the case of only partial thermal redistribution in the secondary cooling zone, the increase in the final austenite grain size with increasing OM depth depends on the casting parameters. For a casting speed of 1.2 m/min, an OM depth of 0.1 mm results in an increase of the grain size by approximately 20 %. For deeper OMs (0.4 mm) the increase of the grain size amounts to 30%. Compared to the influence of the casting speed, the secondary cooling intensity seems to play the more important role for the final grain size. Assuming unrestricted and uniform cooling of the surface in the secondary cooling zone the temperature differences will rapidly be compensated. In this case, the final austenite grain size increases steadily with rising OM depth.

In reality, the heat transfer at the bottom of the oscillation marks will partly be prevented by the sticking of mold powder slag and scale. A significant increase of the austenite grain size is therefore likely.
According to Mintz[1], the minimum of the reduction of area (RA) within the second ductility trough is in inverse ratio with the square root of the grain diameter. An increase of the grain size by 30% will therefore lower RA by approximately 12%. Other authors see the RA as in inverse ratio with the grain diameter [20]. This would result in a decrease of the RA by 23 %. The quantification of these more or less quantitative indications will be part of ongoing research work [21].

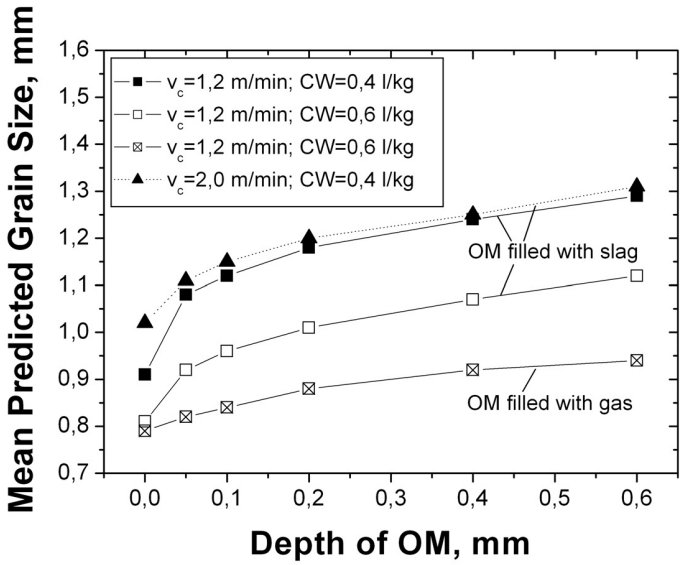

Figure 9: Mean predicted grain size vs. depth of OM for different casting parameters (steel A in table I)

SUMMARY

The present work deals with measurements of austenite grain size on slabs and specimens from laboratory experiments, as well as the adjustment of parameters in a grain size prediction model for the continuous casting process. The grain growth model was coupled with a precipitation model in order to account for the pinning effect of nitrides and carbo-nitrides.
The grain size prediction model allows an accurate description of the experimental results. A clear maximum of the final grain size was found for an equivalent carbon content of between 0.15 and 0.17 wt.-%.
The model was finally applied to the question, how far the formation of oscillation marks at the surface of slabs would result in a local increase of the prior austenite grain size. Under the assumption of partial thermal redistribution, already shallow oscillation marks result in an increase of the prior austenite grain size of up to 20 %, depending on the casting parameters. Thereby the secondary cooling intensity seems to play the most important role. In reality, the grain size difference will be lower as the temperature gradients will partly be compensated. In any way, coarse austenite grains will reduce the ductility of the cast material at temperatures within the second ductility trough. The challenging question how far the ductility is reduced, is part of ongoing research work.

ACKNOWLEDGEMENTS

The authors gratefully acknowledge the support of the Austrian Ministry for Labor and Science and the Christian Doppler Research Association.

REFERENCES

1. B. Mintz, S. Yue and J.J. Jonas, “Hot ductility of steels and its relationship to the problem of transverse cracking during continuous casting,” *International Materials Review*, Vol. 36, 1991, pp. 187-217.
2. R. Dippenaar, S.-C. Moon and E.S. Szekeres, ”Strand Surface Cracks-The Role of Abnormally-Large Prior-Austenite Grains,” *AISTech 2006 Proceedings*, Vol. 1, pp. 833-843.
3. Y. Maehara, H. Tomono and K. Yasumoto, “Effect of Notch Geometry on Hot Ductility of Austenite,” *Trans. ISIJ*, Vol. 27, 1987, pp. 103-109.
4. P. Deprez, J.P. Bricout and J. Oudin, “Tensile test on in situ solidified notched specimens: effects of temperature history and strain rate on hot ductility of Nb and Nb-V-microalloyed steels,” *Mat. Sci. and Engineering*, Vol. A168, 1993, pp. 17-22.

5. Y. Maehara, K. Yasumoto, H. Tomono, T. Nagamichi and Y. Ohmori, "Surface cracking mechanism of continuously cast low carbon low alloy steel slabs," *Materials Science and Technology*, Vol. 6, 1990, pp. 793-805.
6. K. Yasumoto, T. Nagamichi, Y. Maehara and K. Gunji, "Effects of Alloying Elements and Cooling Rate on Austenite Grain Growth in Solidification and the subsequent Cooling Process of Low Alloy Steel," *Tetsu-to-Hagane (J. Iron Steel Inst. Jpn.)*, Vol. 73, no. 14, 1987, pp. 1738-1745.
7. K. Schwerdtfeger, A. Köthe, J.M. Rodriguez and W. Bleck, "Thin slab casting, Volume 1," *EUR 19409/1 EN*, Luxembourg, 2001, pp. 33-48.
8. B. Weisgerber, K. Harste and W. Bleck, "Phenomenological Description of the Surface Morphology and Crack Formation of Continuously Cast Peritectic Steel Slabs," *steel research int.*, Vol. 75, 2004, pp. 686-692.
9. Y. Le Papillon, W. Jaeger, M. Konig, B. Weisgerber and M. Jauhole, "Determination of high temperature surface crack formation criteria in continuous casting and thin slab casting," *EUR 20897 EN*, Luxembourg, 2003.
10. A.K. Giumelli, M. Militzer and E.B. Hawbold, "Analysis of the Austenite Grain Size Distribution in Plain Carbon Steels," *ISIJ International*, Vol. 39, No. 3, 1999, pp. 271-280.
11. J. Reiter, C. Bernhard and H. Preßlinger, "Determination and Prediction of Austenite Grain Size in Relation to Product Quality of the Continuous Casting Process," *Materials Science & Technology (MS&T '06)*, Conference and Exhibition, Cincinnati, USA, October 2006, pp. 805-816.
12. J. Reiter. and C. Bernhard, "Austenite grain size in the continuous casting process: metallographic methods and evaluation," submitted for publication in *Materials Characterization*.
13. Y. Nuri, T. Ohashi, T. Hiromoto and O. Kitamura, "Solidification microstructure of ingots and continuously cast slabs treated with rare earth metal," *Transactions ISIJ*, Vol. 22, 1982, pp. 399-416.
14. P. Ackermann, W. Kurz und W. Heinemann, "In situ tensile testing of solidifying Aluminium and Al-Mg-shells," *Mat. Science and Eng.*, Vol. 75, 1985, pp. 79-86.
15. H. Hiebler, and C. Bernhard, "Mechanical Properties and Crack Susceptibility of Steel during Solidification," *steel research*, Vol. 69, no. 8+9, 1999, pp. 349-355.
16. C. Bernhard, H. Hiebler, and M. Wolf, "Experimental Simulation of Subsurface Crack Formation in Continuous Casting," *Revue de Métallurgie,* Cahiers d'Information Techniques, March (2000), pp. 333-344.
17. Bernhard, C., J. Reiter und H. Presslinger, "A model for predicting the austenite grain size at the surface of continuously cast slabs," submitted for publication in *Metallurgical Transactions B*
18. Andersen, and O. Grong, "Analytical Modelling of Grain Growth in Metals and Alloys in the Presence of Growing and Dissolving Precipitates – I. Normal Grain Growth," *Acta metal. mater.*, Vol 43, 1995, pp. 2673-2688.
19. C. Bernhard und T. Sjökvist, "The interactive continuous casting simulation at www.steeluniversity.org," *Berg- und Huettenm. Mon.*, Vol. 151, No. 5, 2006, pp. 189-195
20. Y. Ohmori and T. Kunitake, "Effects of austenite grain size and grain boundary segregation of impurity atoms on high temperature ductility," *Metal Science*, vol. 17, 1983, pp. 325-332.
21. C. Bernhard, R. Pierer, A. Tubikanec and C. Chimani, "Experimental characterization of crack sensitivity under continuous casting conditions," *Proceedings of the CCR'04 – Continuous Casting and Hot Rolling Conference*, Paper No. 6.3, 14.-15. June 2004, Linz.